Atomic Fock State Preparation Using Rydberg Blockade

Matthew Ebert,* Alexander Gill, Michael Gibbons, Xianli Zhang, Mark Saffman, and Thad G. Walker
Department of Physics, University of Wisconsin, 1150 University Avenue, Madison, Wisconsin 53706, USA
(Received 28 October 2013; published 30 January 2014)

We use coherent excitation of 3–16 atom ensembles to demonstrate collective Rabi flopping mediated by Rydberg blockade. Using calibrated atom number measurements, we quantitatively confirm the expected $\sqrt{N}$ Rabi frequency enhancement to within 4%. The resulting atom number distributions are consistent with an essentially perfect blockade. We then use collective Rabi π pulses to produce $\mathcal{N} = 1$, 2 atom number Fock states with fidelities of 62% and 48%, respectively. The $\mathcal{N} = 2$ Fock state shows the collective Rabi frequency enhancement without corruption from atom number fluctuations.

DOI: 10.1103/PhysRevLett.112.043602 PACS numbers: 42.50.Dv, 03.67.-a, 32.80.Rm, 78.67.-n

Ensembles of cold neutral atoms localized in micron-sized clouds interact collectively with laser light tuned to excite $n \sim 100$ Rydberg states. Within such clouds the interactions between two or more Rydberg atoms are many orders of magnitude greater than the interactions between ground-state atoms. Thus, while a single photonic absorption is resonant, subsequent photonic absorptions are made off resonant by Rydberg-Rydberg interactions. For sufficiently cold atoms, this "blockade" energetically constrains the N atom ensemble to an effective two-level Hilbert space consisting of either N ground-state atoms or $N-1$ ground-state atoms and 1 Rydberg excitation. The sharing of the excitation between the N atoms causes atom-light couplings to be collectively enhanced by $\sqrt{N}$ [1,2].

For $N = 2$, Rydberg blockade [3,4] has been exploited to produce entanglement [5–7] and to observe $\sqrt{2}$ Rabi enhancement [4]. Collective Rabi oscillations at large N were also recently observed [8]. Even when the cloud size allows multiple Rydberg excitations, blockade results in excitation suppression and dramatically increased optical nonlinearities. This works even at the single photon level [9–12] and allows entanglement of light and atomic excitations [13].

The classic signature of coherent collective behavior is collective Rabi flopping, as emphasized in the original Lukin *et al.* proposal [1]. Fluctuations in atom loading statistics produce, through the $\sqrt{N}$ dependence, inhomogeneous broadening that dephases the collective Rabi manipulations. This is important, for example, for potential use in collective quantum gates [14], protocols for deterministic single photon sources [15], or entanglement of single-atom and collective qubits [16]. To minimize this effect, one would like to be able to reduce the atom number fluctuations below the classical Poissonian limit, also proportional to $\sqrt{N}$.

In this Letter we experimentally realize a collective protocol [15] for deterministic production of single- and two-atom Fock states. We load an ensemble of $3 < \bar{N} < 16$ atoms into a single dipole trap and extract single atoms via collective Rabi π pulses between one ground-state hyperfine level and a Rydberg state, followed by stimulated emission into a second ground hyperfine level, Fig. 1(c). We quantitatively verify the $\sqrt{N}$ enhancement factor to within $\pm 4\%$. Subsequent sequences of such pulse pairs allow production of multiatom Fock states. We demonstrate sub-Poissonian production of single- and two-atom Fock states using this method.

Our basic apparatus is quite similar to our previous work [6,7]. Indeed, the collective Rabi flopping protocols are similar to protocols for single-atom qubit control, and hence are convenient for loading arrays for neutral atom quantum computing. We transfer a small number of Rb atoms (up to 30) from a magneto-optical trap into a 1.5 mK deep 1.06 μm far-off resonance trap (FORT) focused to a waist of 3.0 μm. The atoms are then laser cooled to 100–150 μK, during which time light-assisted collisions induced by the cooling light cause atoms to be ejected from the FORT. Varying the cooling time allows us to realize a mean atom number $\bar{N}$ from 0.5 to 16 atoms. Measurement of $\bar{N}$ will be discussed later. The spatial distribution of the trapped atoms is a 7 μm long and < 0.5 μm wide Gaussian distribution oriented along the FORT propagation direction. Calculations indicate that the Rydberg-Rydberg interaction [17] is 11 MHz at a typical 12 μm atom-atom distance, sufficient for the 1 MHz scale Rabi flopping studied here. Once trapped, the atoms are optically pumped into the $|5S_{1/2}, F = 2, m_F = 0\rangle$ clock state, and the FORT is turned off for 3–6 μs while the Fock state pulse sequence is applied.

The Fock state pulse geometry is shown in Fig. 1(a). We perform independent coherent two-photon excitations between either of the two ground states $(|a\rangle, |b\rangle) = |5S_{1/2}, F = (2,1), m_F = 0\rangle$ and the $|r\rangle = |97D_{5/2}, m_J = 5/2\rangle$ Rydberg state. Two independently switchable 780 nm lasers, with waists of $\omega_{(x,y)} = (9,7)$ μm, energetically select the hyperfine level coupled to $|r\rangle$. Both of these lasers copropagate with the FORT laser. A counterpropagating 480 nm beam with waists of $\omega_{(x,y)} = (5.6, 4.7)$ μm, which is left on continuously, provides the second step to

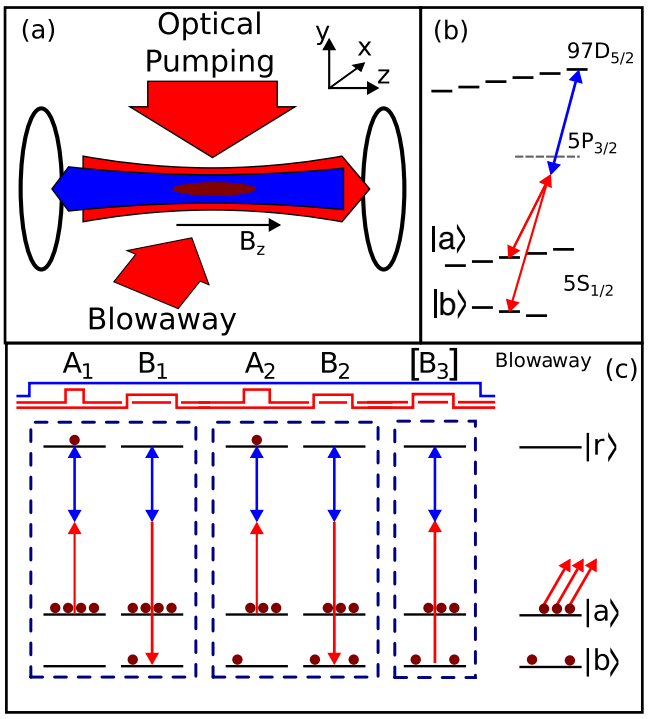

FIG. 1 (color online). (a) Experimental geometry. Counter-propagating 780 and 480 nm Rydberg excitation lasers, parallel to an applied magnetic field, couple $|a\rangle$ or $|b\rangle$ to $|r\rangle$. Optical pumping and state selective blowaway beams are incident on the ensemble in the perpendicular plane. (b) Two-photon excitation diagram. (c) Fock state generation pulse sequences. Sequential pairs of A and B excitation pulses perform population transfer from $|a\rangle \rightarrow |r\rangle \rightarrow |b\rangle$. Ideally, the Rydberg blockade mechanism moves a single atom to $|b\rangle$ per A-B pulse pair. After two A-B pulse pairs, the B_3 pulse optionally probes two-atom Fock state dynamics.

the Rydberg state. Each excitation laser is locked to a different mode of a high finesse cavity. The single-photon Rabi frequencies for the two-photon transition are typically $(\Omega_{480}, \Omega_{780}) = 2\pi \times (17, 160)$ MHz, with a -2.1 GHz detuning from the $5P_{3/2}$ level, giving a single-atom two-photon Rabi frequency of $\Omega_1 = 2\pi \times 750$ kHz. The timing of each pulse is controlled by the duration of the respective 780 nm beams. In the following, we refer to a Rabi oscillation between $(|a\rangle, |b\rangle)$ and $|r\rangle$ as an (A_p, B_p) pulse, where p refers to the pulse sequence number in Fig. 1(c). All pulse times t are chosen to have pulse area $\theta = \pi = \sqrt{\bar{N}}\Omega t$, unless explicitly noted.

Following the Fock state pulses, the number ($N_b = 0$, 1, or 2) of atoms in state $|b\rangle$ is determined by first ejecting atoms from $|a\rangle$ using resonant light [6], then collecting light from the remaining atoms while laser cooling for 20 ms. Measurements show that atoms in $|a\rangle$ can be ejected with a fidelity of 97%. Atoms remaining in Rydberg states at the end of a pulse sequence leave the trap after the FORT is turned back on [3], so population in Rydberg states is not directly detected in this experiment.

Beginning with an $\bar{N}$ atom ensemble initialized in $|a\rangle$, the $A_1(\theta)$ pulse produces a collective Rabi oscillation between the state $|g\rangle = |a_1 a_2 \ldots a_N\rangle$ and the symmetric singly excited W state $|r\rangle = N^{-1/2} \sum_{i=1}^{N} |a_1 a_2 \ldots r_i \ldots a_N\rangle$. The B_1 pulse, calibrated using single-atom Rabi oscillations out of state $|b\rangle$, then drives a single-atom π pulse between the single Rydberg atom and the unpopulated $|b\rangle$ state. Ideally, this sequence should produce a single-atom Fock state in $|b\rangle$.

Figure 2 shows the results of measurements of N_b after $A_1(\theta)B_1$ sequences. As the number of atoms is successively increased from 1 (top) to 15.5 (bottom), the Rabi frequency increases as expected from collective enhancement. We fit each data set to the following model for the probability $p_1(t)$ for one atom to be in $|b\rangle$ as a function of $A_1(\theta)$ pulse time:

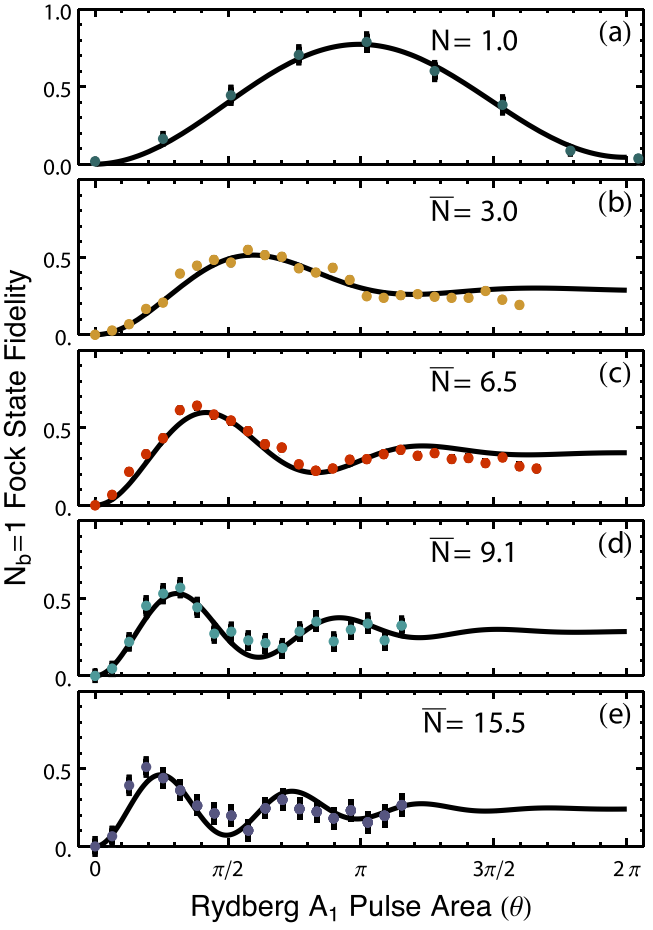

FIG. 2 (color online). Rabi oscillations between $|a\rangle$ and $|r\rangle$ for various atom number distributions. The single-atom detection probability is shown as a function of the pulse area $\theta = \Omega_1 t$ of the Rydberg A excitation. (a) The first 2π rotation for exactly one atom. A π pulse takes 670 nsec. (b)–(e) The $|b\rangle$ populations show an atom number dependent frequency for ensemble means of, respectively, $\bar{n} = 3.0$, 6.5, 9.1, 15.5. The solid black lines are the fits to Eq. (1).

$$p_1(t) = \frac{\epsilon}{2}\sum_{N=0}^{\infty} P_{\bar{N}}(N)[1-\cos(\sqrt{N}\Omega_1 t)e^{-t/\tau}], \quad (1)$$

where $P_{\bar{N}}(N)$ is the Poisson distribution of initial atom numbers and τ is the decay time of the Rabi oscillations. Both Ω_1 and τ (typically $2\pi \times 750$ kHz and 5 μs) are measured from single-atom Rabi flopping. A two-parameter fit for each data set returns the mean atom number $\bar{N}$ and an overall scaling factor ϵ, to be discussed with Fig 5.

We separately measure $\bar{N}$ by collecting fluorescence scattered by the atoms from short (3 ms) pulses of cooling light. In the $> 10^{11}$ cm^{-3} density cloud, the calibration of the number of scattered photons per atom is affected by significant light-assisted collision loss. In separate experiments we measure the relevant two-body loss rates and implement the relevant calibrations [18].

A comparison between $\bar{N}$ as deduced from the collective Rabi oscillations, and from the direct atom number measurements, is shown in Fig. 3, along with a line of slope 1. The close agreement quantitatively confirms the phenomenon of collective Rabi frequency enhancement in the strong blockade limit. Allowing the slope to vary gives a best fit of 0.96 ± 0.04.

Figure 2 demonstrates that when the Rydberg A_1 pulse area is chosen to be a collective π pulse, i.e., $\Omega_{\bar{N}} t = \pi$, and the Rydberg B_1 pulse is set to a single atom π pulse, our procedure is capable of creating an $\mathcal{N} = 1$ Fock state in which a single atom of the ensemble has been transferred to the state $|b\rangle$ with an efficiency as high as 63.3% at $\bar{N} = 6$. The observed distribution of N_b is 35% $N_b = 0$, 63.3% $N_b = 1$, and 1.3% $N_b = 2$. The number of $N_b = 2$ cases observed is consistent with our known efficiency for ejecting the atoms in $|a\rangle$, implying that any double Rydberg excitations due to imperfect blockade do not transfer to $|b\rangle$. The resulting Fock state distribution is very sub-Poissonian with a Mandel parameter $Q = \sigma^2_{N_b}/\bar{N}_b - 1 = -0.62 \pm 0.03$.

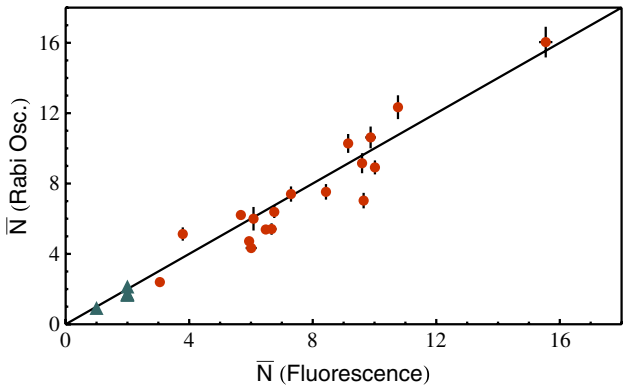

FIG. 3 (color online). Mean number of atoms in the ensemble, as deduced from collective Rabi oscillations (ordinate) and by fluorescence (abscissa). The red circles are data from Poisson-distributed atom ensembles, the green triangles have exactly 1 or 2 atoms. The solid black line, of slope 1, shows that the collective oscillation frequency closely follows the predicted $\sqrt{N}$ dependence.

The $\mathcal{N} = 1$ Fock state preparation procedure can be generalized to $\mathcal{N} > 1$ by simply repeating the Rydberg A and B pulse sequence $\mathcal{N}$ times, with each pulse area set to be a collective π pulse for the number of coupled atoms. Thus, the ideal collective Rabi frequencies for pulses A_2 and B_2 are $\sqrt{\bar{N}-1}\Omega_1$ and $\sqrt{2}\Omega_1$. To study $\mathcal{N} = 2$ Fock state preparation, we first consider the possible outcomes of an A_1B_1 pulse sequence followed by an A_2 pulse. There are four cases $|N_r, N_b\rangle$: (1) neither pulse sequence succeeds: $|0,0\rangle$; (2) A_1B_1 succeeds but A_2 fails, resulting in one atom in $|b\rangle$: $|0,1\rangle$; (3) A_1 fails and A_2 succeeds, resulting in one Rydberg atom: $|1,0\rangle$; (4) all pulses succeed, resulting in one atom in both $|b\rangle$ and $|r\rangle$: $|1,1\rangle$. Finally, a fourth pulse, $B_2(\theta)$, couples $|b\rangle \leftrightarrow |r\rangle$ and evokes different behavior for each possible state mentioned. For $|0,0\rangle$, B_2 has no effect. Both single-atom outcomes oscillate between $|0,1\rangle \leftrightarrow |1,0\rangle$ at the single-atom Rabi frequency but are out of phase with each other. The $|1,1\rangle$ state, however, uniquely oscillates between $|1,1\rangle \leftrightarrow |0,2\rangle$ at a $\sqrt{2}\Omega_1$ enhanced Rabi frequency. Blockade forbids population of $|2,0\rangle$, and, in particular, does not allow the atoms to simply interchange $b \leftrightarrow r$. The population of the $|b\rangle$ state will then be either 0, 1, or 2 atoms.

Figure 4(a) shows the probabilities for observing 0, 1, or 2 atoms in state $|b\rangle$ after the $A_1B_1A_2B_2(\theta)$ sequence. As expected, the probability of observing two atoms, Fig. 4(a2), begins at 0 and oscillates at $\sqrt{2}\Omega_1$. Note that the decay time of the two-atom collective oscillation is set by the same decoherence processes as would be observed in single atom-atom Rabi oscillations, and there is no additional dephasing from atom number fluctuations because exactly two atoms participate in the oscillation. The $N_b = 0$ signal, Fig. 4(a0), potentially has contributions from the single-atom states $|0,1\rangle$ and $|1,0\rangle$, but these oscillations are

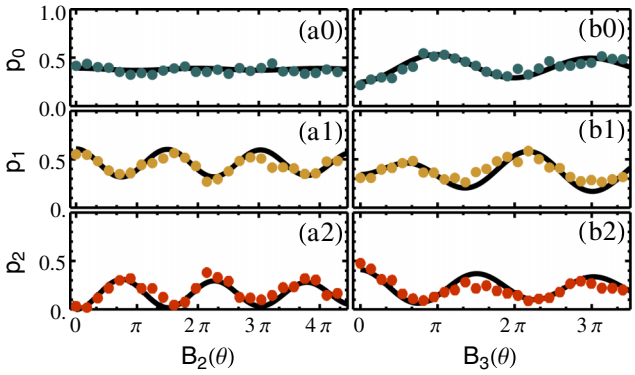

FIG. 4 (color online). (a) Evolution of $N_b = 0$, 1, and 2 atom populations using the $A_1B_1A_2B_2(\theta)$ protocol. (b) Output of the $\mathcal{N} = 2$ Fock state production as a function of B_3 area.

out of phase and cancel if the populations of those states are equal, as is nearly the case for this data.

The $N_b = 1$ signal, Fig. 4(a1), potentially has contributions from Rabi oscillations of the states ($|1,0\rangle$, $|0,1\rangle$, $|1,1\rangle$) at frequencies $(1, 1, \sqrt{2})\Omega_1$. Again, the first two are canceled if their populations are equal, leaving only the collective two-atom signal.

The probability of producing the Fock state $|0,2\rangle$ is 32% for this data, for which the FORT drop time was extended to 6.34 μs to see three full collective Rabi oscillations. As a result, additional high velocity atoms are not recaptured when the FORT is restored, reducing the signal size. For 2 μs FORT drops, we have observed up to $48 \pm 2\%$ $N_b = 2$. For example, the state produced at the beginning of Fig. 4(b) has $Q = -0.50 \pm 0.05$.

The full $F = 2$ Fock sequence can be further probed by restoring the FORT for 0.5 ms, enough to eject any Rydberg population from $|1,0\rangle$ and $|1,1\rangle$, effectively leaving only ground-state populations in the states $|0,0\rangle$, $|0,1\rangle$, and $|0,2\rangle$. This removes the cancellation between the $|0,1\rangle$ and $|1,0\rangle$ signals observed in Fig. 4(a). Now, as shown in Fig. 4(b), oscillations at Ω_1 are observed in the $N_b = 0$ data, and the $N_b = 1$ data have both Ω_1 and $\sqrt{2}\Omega_1$ signals superposed. The fits to the oscillations have only the three initial state populations as adjustable parameters, and assume no atom number fluctuations.

Both the $N_b = 1$ and $N_b = 2$ Fock state populations are consistent with a single collective AB sequence success probability of 0.65–0.70. In Fig. 5 we show the $\mathcal{N} = 1$ Fock state population as a function of $\bar{N}$. We also show the results of a quantum Monte Carlo model of a collective A_1B_1 pulse sequence. The model considers the known significant sources of experimental imperfections, which include Doppler shifts, the distribution of ac-Stark shifts and Rabi frequencies from the Gaussian intensity distributions, spontaneous emission from the intermediate $5p$ state (spontaneous emission from the Rydberg states is negligible on 5 μs time scales), and 1 μm misalignments of the excitation lasers. For a single atom, the model reproduces our observed AB success probability of 85%. For multiple atoms, the model allows both single and double Rydberg excitations. The double excitations during the A portion of the sequence primarily consist of atom pairs at extreme ends of the cloud. Those double excitations still experience some Rydberg-Rydberg interactions, and therefore are off resonant for the B deexcitation portion of the sequence, thereby suppressing the number of occurrences of $N_b = 2$. The lines in Fig. 5 show, from highest to lowest, the predicted fidelity assuming perfect Rabi flopping and infinite blockade, experimental imperfections with infinite blockade, and finally including both experimental imperfections and finite blockade. The black dashed curve corresponds to the fit parameter $\epsilon = 1$ in Eq. (1).

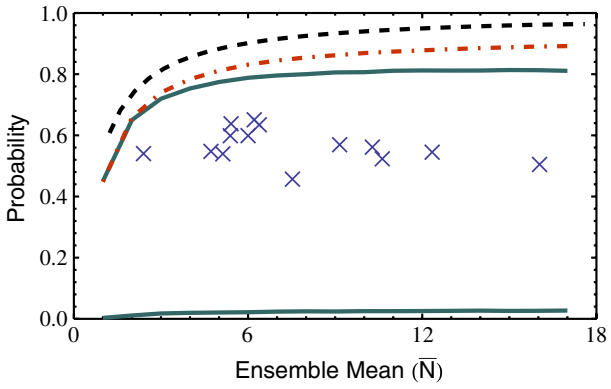

FIG. 5 (color online). $\mathcal{N} = 1$ Fock state production fidelity as a function of mean ensemble number and quantum Monte Carlo simulations. The black dashed line assumes ideal blockade and perfect excitation conditions. The red dot-dashed line adds in realistic experimental imperfections, and the green solid line includes finite blockade strength. The solid green line at the bottom shows the predicted two-atom production.

Using this information, the predicted Fock state sequence fidelity should reach 80% by $\bar{N} = 7$. This is 15% higher than we observe in the experiment, and gets slightly worse with increasing $\bar{N}$. The source of the additional inefficiency is unknown to us, but we note that our densities, $5N \times 10^{10}$ cm^{-3}, approach peak densities where laser cooling limits are observed due to multiple scattering. We note that recent results on using Rydberg blockade for single-photon sources [8] found a $67 \pm 10\%$ preparation efficiency of the singly excited many-body state at similar atom densities.

The Q parameter for deterministic $\mathcal{N} = 1$ schemes studied to date give collisional blockade using light-assisted collisions, $Q = -0.5$ [19,20], this work, $Q = -0.65$, repulsive light-assisted collisions, $Q = -0.91$ [21], and Mott-insulator samples, $Q = -0.95$ [22]. For $\mathcal{N} = 2$ with $Q = -0.5$, other methods to date require cooling to quantum degeneracy: the $\mathcal{N} = 2$ shell of a Mott insulator [22], or controlled spilling from a degenerate Fermi gas [23]. Both achieve $Q < -0.9$.

Our studies of Rydberg-blockade-mediated collective Rabi flopping show that the collective Rabi frequencies very closely follow the predicted $\Omega_N = \sqrt{N}\Omega_1$ dependence. This, plus our observation of the lack of two-atom production in an A_1B_1 sequence, strongly imply that the blockade phenomenon is highly effective at rejecting double Rydberg excitations. We used the collective flopping to produce a strongly sub-Poissonian atom distribution with $Q = -0.65$ in a single trap site. Extending the protocol to a two-atom Fock state, we get $Q = -0.5$ and observe three cycles of $N = 2$ collective Rabi flopping with no additional dephasing. Future plans include producing blockaded samples with higher numbers of atoms at lower densities, where possible density dependent mechanisms should be lessened.

Important contributions at early stages of this work were made by Erich Urban, Thomas Henage, and Larry

Isenhower, and we acknowledge helpful discussions with Klaus Mølmer. This work was funded by NSF Grant No. PHY-1104531 and the AFOSR Quantum Memories MURI.

*mebert@wisc.edu

[1] M. D. Lukin, M. Fleischhauer, R. Cote, L. M. Duan, D. Jaksch, J. I. Cirac, and P. Zoller, Phys. Rev. Lett. **87**, 037901 (2001).
[2] M. Saffman, T. G. Walker, and K. Mølmer, Rev. Mod. Phys. **82**, 2313 (2010).
[3] E. Urban, T. A. Johnson, T. Henage, L. Isenhower, D. D. Yavuz, T. G. Walker, and M. Saffman, Nat. Phys. **5**, 110 (2009).
[4] A. Gaëtan, Y. Miroshnychenko, T. Wilk, A. Chotia, M. Viteau, D. Comparat, P. Pillet, A. Browaeys, and P. Grangier, Nat. Phys. **5**, 115 (2009).
[5] T. Wilk, A. Gaëtan, C. Evellin, J. Wolters, Y. Miroshnychenko, P. Grangier, and A. Browaeys, Phys. Rev. Lett. **104**, 010502 (2010).
[6] L. Isenhower, E. Urban, X. L. Zhang, A. T. Gill, T. Henage, T. A. Johnson, T. G. Walker, and M. Saffman, Phys. Rev. Lett. **104**, 010503 (2010).
[7] X. L. Zhang, L. Isenhower, A. T. Gill, T. G. Walker, and M. Saffman, Phys. Rev. A **82**, 030306(R) (2010).
[8] Y. O. Dudin, L. Li, F. Bariani, and A. Kuzmich, Nat. Phys. **8**, 790 (2012).
[9] T. Peyronel, O. Firstenberg, Q.-Y. Liang, S. Hofferberth, A. V. Gorshkov, T. Pohl, M. D. Lukin, and V. Vuletic, Nature (London) **488**, 57 (2012).
[10] Y. O. Dudin and A. Kuzmich, Science **336**, 887 (2012).
[11] D. Maxwell, D. J. Szwer, D. Paredes-Barato, H. Busche, J. D. Pritchard, A. Gauguet, K. J. Weatherill, M. P. A. Jones, and C. S. Adams, Phys. Rev. Lett. **110**, 103001 (2013).
[12] J. Honer, R. Löw, H. Weimer, T. Pfau, and H. P. Büchler, Phys. Rev. Lett. **107**, 093601 (2011).
[13] L. Li, Y. O. Dudin, and A. Kuzmich, Nature (London) **498**, 466 (2013).
[14] I. I. Beterov, M. Saffman, E. A. Yakshina, V. P. Zhukov, D. B. Tretyakov, V. M. Entin, I. I. Ryabtsev, C. W. Mansell, C. MacCormick, S. Bergamini, and M. P. Fedoruk, Phys. Rev. A **88**, 010303(R) (2013).
[15] M. Saffman and T. G. Walker, Phys. Rev. A **66**, 065403 (2002).
[16] M. Saffman and T. G. Walker, Phys. Rev. A **72**, 042302 (2005).
[17] T. G. Walker and M. Saffman, Phys. Rev. A **77**, 032723 (2008).
[18] See Supplemental Material at http://link.aps.org/supplemental/10.1103/PhysRevLett.112.043602 for a description of the atom ensemble florescence calibration.
[19] M. T. DePue, C. McCormick, S. L. Winoto, S. Oliver, and D. S. Weiss, Phys. Rev. Lett. **82**, 2262 (1999).
[20] N. Schlosser, G. Reymond, and P. Grangier, Phys. Rev. Lett. **89**, 023005 (2002).
[21] A. V. Carpentier, Y. H. Fung, P. Sompet, A. J. Hilliard, T. G. Walker, and M. F. Andersen1, Laser Phys. Lett. **10**, 125501 (2013).
[22] W. S. Bakr, A. Peng, M. E. Tai, R. Ma, J. Simon, J. I. Gillen, S. Fölling, L. Pollet, and M. Greiner, Science **329**, 547 (2010).
[23] F. Serwane, G. Zürn, T. Lompe, T. B. Ottenstein, A. N. Wenz, and S. Jochim, Science **332**, 336 (2011).

Atomic Fock State Preparation Using Rydberg Blockade
Supplementary Material

Matthew Ebert,* Alexander Gill, Michael Gibbons, Xianli Zhang, Mark Saffman, and Thad G. Walker
Department of Physics, University of Wisconsin,
1150 University Avenue, Madison, Wisconsin 53706, USA
(Dated: January 2, 2014)

LIGHT-ASSISTED COLLISION RATE CALIBRATION

A quantitative analysis of the collective frequency enhancement requires an initial atom number measurement. In the absence of light-assisted collisions, the distribution of collected fluorescence counts s for N atoms after time t would be a Gaussian distribution $G_N(s,\bar{s})$ with a mean $\bar{s} = N\Gamma t$ and a standard deviation $\sigma_N = \sqrt{\bar{s}}$. Here Γ is the single-atom photon detection rate, typically 8-9 photons/ms, so that with > 3 ms of detection time the assumed Gaussian distribution is a good approximation to the actual Poisson distribution.

Interpretation of fluorescence measurements is complicated by significant two-body loss from light-assisted collisions over ms timescales. Since this loss rate is roughly proportional to N^2, large atom numbers will be significantly underestimated, as illustrated in Figure 1(a). To this end, we measure and account for the two-body losses.

The probability p_N of finding atom number N is given by the differential equation

$$\frac{dp_N}{dt} = \frac{\beta}{2}\left[(N+2)(N+1)p_{N+2}(t) - N(N-1)p_N(t)\right], \quad (1)$$

$$p_N(0) = P_{\bar{N}}(N) \quad (2)$$

where β is the two-body loss rate, and $P_{\bar{N}}(N)$ is the Poisson distribution at N with mean $\bar{N}$.

For large $\bar{N}$ such that after the exposure time there is a small probability of being left with the asymptotic values of 0 (even) or 1 (odd) samples, we use the simplified continuous model given by:

$$\frac{d\bar{N}(t)}{dt} = -\beta\bar{N}(t)\left(\bar{N}(t) - 1\right), \quad (3)$$

Then the mean camera signal, $\bar{s}$, generated by an initial mean $\bar{N}$ atoms, during an integration time t is given by:

$$\bar{s}(\bar{N},t) = \frac{\Gamma}{\beta}\ln\left[1 + \left(e^{\beta t} - 1\right)\bar{N}\right], \quad (4)$$

By fitting the camera signal to Equation (4) we deduce β and $\bar{N}$. An example is shown in Figure 1(a).

We estimate the accuracy of our mean number determination to be ±3%. This includes typical 2% uncertainty in the fit parameters for the camera signal (Fig. 2b), a 1% uncertainty in Γ, and a 1% uncertainty in the fit of β from Fig. 2a.

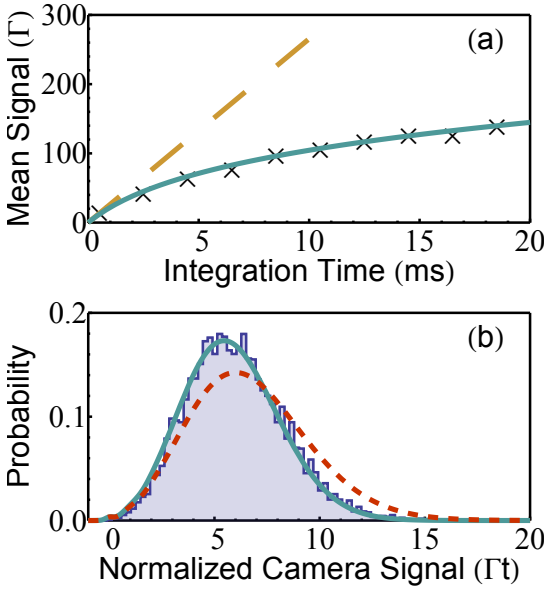

FIG. 1. (a) The integrated camera signal is shown along with the fit (solid green) to Eq. (4). The best fit parameters are $\bar{n} = 26.5$ and $\beta = 0.0170/(\text{atom ms})$. The camera signal in the ideal case of no two-body loss is shown as the dashed yellow line to demonstrate the magnitude of the light-assisted collision effect. (b) An example camera signal distribution is shown (blue bars), with a fit to Eq. (5) (solid green) using $\beta = 0.0158/(\text{atom ms})$ giving $\bar{N} = 6.68$ atoms, as compared to the expected distribution in the limit of no loss (dashed red).

MULTIATOM MEASUREMENTS

Once β is known, and assuming Poisson loading statistics, the mean atom number can be measured with a fixed camera integration time short enough so that $\bar{s}(N,t)$ is still close to linear in time. The resulting camera signal in bin s is a Poisson weighted sum of Gaussian distributions centered around the mean signals $\bar{s}(N,t)$ for N atoms:

$$\bar{S}(s) = \sum_{N=0}^{N=n_f} P_{\bar{N}}(N)G_N(s,\bar{s}(N,t)) \quad (5)$$

where σ_0 is the background signal standard deviation. For our normal 3 ms integration time $\sigma_0 = 0.188$ atoms and $\sigma_1 = 0.448$ atoms. The only free parameter in the

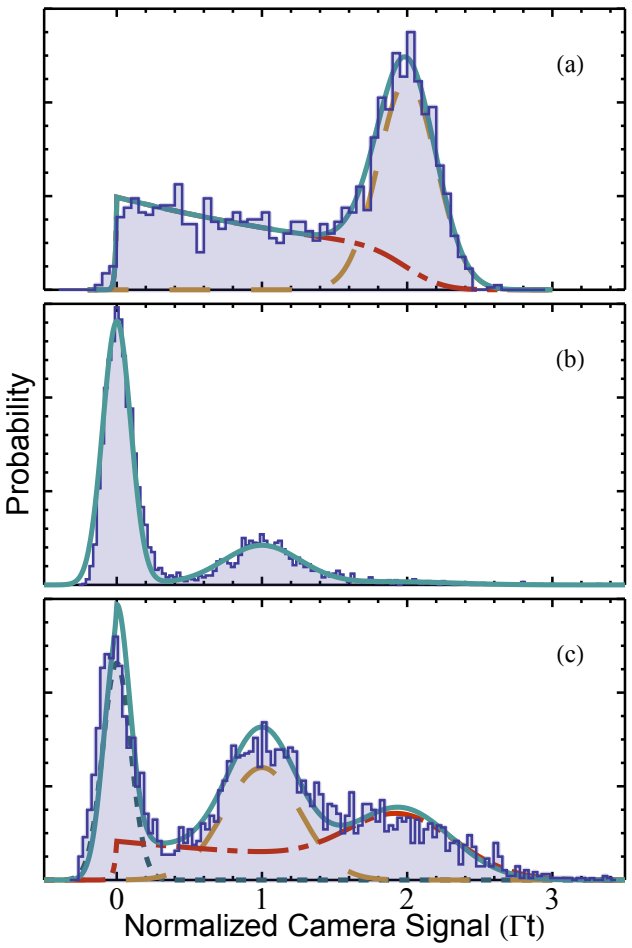

FIG. 2. (a) A Monte Carlo simulation of readout signals observed for a two-atom cloud, including two-body losses, and compared to our analytical model of Eq. (7). (b) A normal single atom readout with 10 ms exposure with minimal two atom signal. (c) An example of $\mathcal{N} = 2$ Fock State data with significant number of two atom occurances. The individual atom signal components are shown for comparison. Note that the gap between the background and 1 atom peaks is not preserved due to the "tail" of the 2 atom distribution from the two body loss.

fit is the Poisson mean $\bar{N}$. An example data set and fit are shown in Figure 1(b).

For longer exposure times, the signal distribution distorts from 2-body losses. This is important for $N < 3$ where long exposure times are needed to get sufficient signal. It is also important for small N to deduce the atom number distribution, as that allows us to isolate single-atom and two-atom Rabi flopping.

When $N = 0, 1$ there is no two-body loss so both signal distributions are Gaussian. When $N = 2$ there are two possible outcomes:

1. no collision occurs so both atoms scatter for the full readout time. This has a probability $e^{-2\beta t}$;
2. a two-body collision occurs and the atoms are ejected at time t' with a probability $e^{-2\beta t'}dt'$.

The signal due to no loss event is Gaussian, whereas for a loss event during the readout the two atoms scatter photons until the loss occurs. This gives a signal distribution

$$G_2^\star(s,t) = \int_0^t dt' e^{-2\beta t'} G_2(s, 2\Gamma t'). \tag{6}$$

We have neglected a small correction in $G_2^\star$ from the background counts, which slightly smear the data near $s = 0$, as seen in Fig. 2(a). The resulting model for the $N \leq 2$ camera distribution $S(s,t)$ is therefore

$$\begin{aligned} S(s,t) = {} & p_0 G_0(s,0) + p_1 G_1(s,\Gamma t) \\ & + p_2 \left[e^{-2\beta t} G_2(s, 2\Gamma t) + (1 - e^{-2\beta t}) G_2^*(s,t) \right]. \end{aligned} \tag{7}$$

To illustrate the effects of light-assisted collisions on the signals, we show in Fig. 2(a) a Monte Carlo simulation of a $p_2 = 1$ distribution, compared to the model. The observed signal distribution for the combined case of 0,1 and 2 atoms is shown in Fig. 2(c). An integration time of $t = 10$ ms was chosen to minimize the overlap integral between the single and double atom distributions. For this integration time, $\sigma_0 = 0.0883$ atoms, $\sigma_1 = 0.236$ atoms.